

Can Strong-Motion Observations be Used to Constrain Probabilistic Seismic-Hazard Estimates?

by C. Beauval, P.-Y. Bard, S. Hainzl, and P. Guéguen

Abstract Because of the new regulatory requirements that hazards have to be estimated in probabilistic terms, the number of probabilistic hazard studies conducted has recently been increasing. The present study aims at defining the possibilities and limits for comparing predictions from these studies and observations. Comparison tests based directly on the rate of ground-motion occurrences are favored over the rate of earthquake occurrences. Based on the properties of Poisson processes, the minimum time window ensuring reliable occurrence rate estimates at a site is computed and evaluated. For example, for ground motions with a 475-yr return period at a site, a minimal 12,000-yr observation time window is required for estimating the rate with a 20% uncertainty (coefficient of variation: standard deviation divided by the mean). These values are not dependent on the seismicity level of the regions under study. An analysis of recorded ground motions at the stations of the permanent French accelerometer network shows that at best, the occurrence rates can be estimated with an accuracy of 30% for very low acceleration levels (0.0001–0.001g for the station STET). The same analysis, carried out at two stations with longer recording histories and located in higher seismicity regions (Greece and California), provides ground-motion levels up to 0.1g. Therefore, the question posed is can the results of a comparison test at low acceleration levels be generalized to higher acceleration levels, even if using a ground-motion prediction equation uniformly valid for a wide range of accelerations?

Introduction

Because of the new regulation requirements that hazards be estimated in probabilistic terms (e.g., recommendations in Eurocode 8 for the European Union), the number of probabilistic hazard studies has recently been increasing. In particular, the seismic zoning in France, applied in the new building code, is for the first time based on probabilistic methodologies (Sollogoub *et al.*, 2007). Several countries like Japan (Fujiwara *et al.*, 2005) have also recently published their first national seismic hazard map based on a probabilistic approach. The consequence of a greater interest in this subject is the multiplicity of hazard estimations, which sometimes contradict each other. For example, at least three different probabilistic studies at a national scale for France have been produced in the last 8 yr (Dominique *et al.*, 1998; Martin *et al.*, 2002; Marin *et al.*, 2004). As a probabilistic seismic hazard map is the result of decisions taken by experts on the choice of models, these discrepancies are not surprising and can be explained (see Sollogoub *et al.*, 2007 for an analysis for France, and Beauval and Scotti, 2004 for a study on the impact of parameter choices). However, these discrepancies raise controversial discussions when probabilistic maps are to be translated into official zoning maps. A record

of such issues and discussions may be found in Humbert *et al.* (2007), Labbé (2007a,b,c), Sollogoub *et al.* (2007), and in Viallet *et al.* (2007). One possibility to reconcile diverse opinions is to try to use available observations to constrain hazard estimates. The present study was initiated in this context; it aims at defining the possibilities and limits for comparing predictions from probabilistic seismic hazard maps and recorded strong ground motions. As expected, the main difficulty is the lifetime of strong-motion networks.

A probabilistic study requires determining the probabilities of occurrence of earthquakes and later the probabilities of occurrence of ground motions. Validation tests have been performed at both levels. For example, McGuire (1979) compared observed and predicted earthquake occurrence rates for the well-documented historical catalog of China; Musson (2004) investigated the fit between seismicity models and spatial earthquake distributions in Great Britain. At the level of ground motions, there have been only a few attempts. Anoohehpour *et al.* (2004) developed a technique using precarious rocks for constraining the levels of ground motion that could have occurred during the time the rocks have been in their current positions. This technique is a key tool for

constraining maximum possible ground motions, but does not deal with occurrence probabilities. Ward (1995) tested occurrence probabilities of calculated accelerations against probabilistic estimations, these calculated accelerations being obtained by combining the historical earthquake catalog with a ground-motion prediction equation. To our knowledge, the only published work presenting a comparison test based on recorded strong motions is by Ordaz and Reyes (1999). Note that in an unpublished work, Tormann *et al.* (2004) performed a similar study at the sites of the New Zealand strong-motion network. The present study builds on these previous results. We favor prediction tests based directly on ground motions rather than on earthquake occurrences. The reason is twofold. First, the aim of probabilistic hazard studies is the computation of the probabilities of occurrence of ground motions (not earthquakes). Secondly, the link between inputs (earthquakes) and outputs (ground motions) is far from straightforward, as will be shown using disaggregation studies in space and recurrence intervals. Most probabilistic seismic hazard studies assume a Poissonian occurrence for earthquakes and ground motions. In this article, we will compare the probabilistic hazard curve with observed annual rates of occurrence, exactly like Ordaz and Reyes (1999) have done for an instrumented site in Mexico City. As all instrumented sites have only been operating for a limited time, at best several decades, our study proposes to determine the minimum time window required at a site for the reliable estimation of a given annual occurrence rate. Applications at several strong-motion stations in France, Greece, and southern California define the acceleration range where the comparison test can be performed.

Back to Basics: Poisson Process and Return Period

The term return period is used extensively when dealing with probabilistic results and hazard maps. It is worth going back to its true meaning and implications before trying to figure out if observations can constrain predictions.

The Poisson hypothesis is widely assumed in the probabilistic seismic hazard framework (Cornell, 1968; Cornell and Winterstein, 1988). An estimation of the probabilistic seismic hazard at a site requires an exhaustive description of the seismic potential of the region: locations, magnitudes, and times of occurrence of future earthquakes. Depending on the level of knowledge regarding the seismicity of a region, some of the sources will be active faults, whereas diffuse seismicity will be taken into account in areal zones (background seismicity). To determine the magnitudes and frequencies of future earthquakes inside the seismic sources, the magnitude recurrence is generally described by a Gutenberg–Richter relation (Gutenberg and Richter, 1944) except when the characteristic model is applied to a fault (Youngs and Coppersmith, 1985; Wesnousky, 1994). Moreover, determining the probabilities of occurrence of earthquakes over future time windows requires a model describing earthquake occurrence in time. Usually the Poisson model is used. This

statistical model implies that earthquakes are independent and occur randomly in time; only mainshocks must be taken into account. A previous study demonstrated that taking into account short-term time dependence in the probabilistic estimation has a low impact on hazard estimates (Beauval *et al.*, 2006a). This might not be the case for long-term time dependence. However, these complex models can be rarely implemented because they require the faults to be very well known (magnitude and date of last earthquake(s) and distribution of interevent times; see, e.g., Working Group on California Earthquake Probabilities (WGCEP), 2003). Therefore, even when seismicity models consist of faults and areal sources, the main model used is the Poisson model. The ground motions produced by these earthquakes are predicted using a ground-motion prediction equation (see Douglas, 2003, for a review). The model describing occurrences in time of earthquakes naturally becomes the model for occurrences in time of ground motions at a site. Thus, the acceleration occurrences (and therefore the acceleration exceedances) are assumed to follow a Poisson process, and the results of a probabilistic study are usually expressed in terms of mean return periods, the inverse of mean annual rates.

A probabilistic study yields the ground motion A^* with a return period T at the site of interest. The return period of reference in the engineering community is still 475 yr (for conventional buildings), so let us show an example for this value. Note that the choice of this return period is historical and basically arbitrary (Bommer and Pinho, 2006) and that engineering design is currently moving to longer return periods (Bommer, 2006), which indeed puts even more emphasis on the validation issue addressed here. A return period of 475 yr corresponds to a 10% probability of exceedance of A^* over 50 yr, which is conventionally considered as the mean lifetime of buildings. The corresponding mean annual rate is ~ 0.0021 or one occurrence on average every 475 yr. For a Poisson process, the probability of having k occurrences over a time window of $t = T$ yr, chosen to be equal to the return period T , is given by $p(k)$:

$$p(k) = \frac{e^{-t/T} (t/T)^k}{k!} = \frac{e^{-1}}{k!}. \quad (1)$$

To understand the implications in terms of frequencies of occurrence, this Poisson process is simulated stochastically (Fig. 1). Numbers of occurrences in time windows of 4750-yr duration are generated. The simulations show that the number of occurrences of an $A \geq A^*$ over a time window equal to T is rarely higher than 4. According to these simulations, if 100 successive time windows were available at the site (equivalent to an observation period of 47,500 yr), we would have 28 time windows without any acceleration exceeding A^* at the site, 48 windows with 1 exceedance, 14 windows with 2 exceedances, and 5 windows with more than 2 exceedances (Fig. 1b). Note that theoretically (equation 1 and Fig. 1b), for a Poisson process with mean 1.0, the probability that the event does not occur over 475 yr is $\sim 37\%$, the

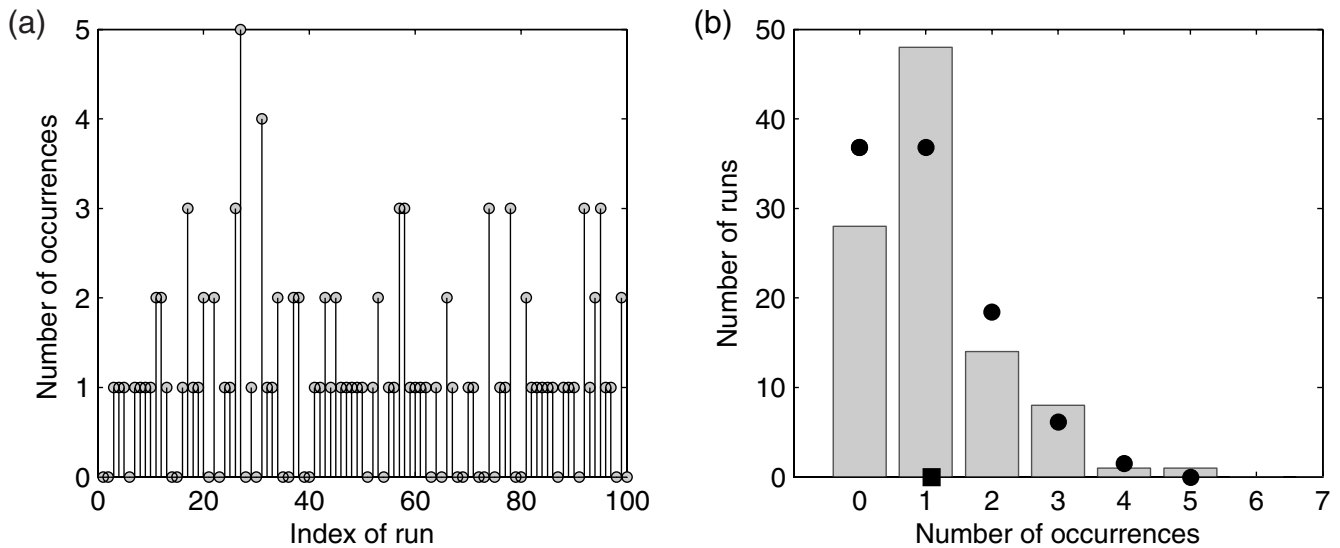


Figure 1. Simulations of a Poisson process with return period 475 yr over time windows of 475 yr. (a) Numbers of occurrence of the event over 100 time windows. (b) Distribution of the 100 values. Square, mean value; plain circles, theoretical values.

probability that it occurs once is $\sim 37\%$, twice is $\sim 18\%$, and more than twice is $\sim 5\%$. This example demonstrates that the ground motion corresponding to a return period of 475 yr is a very rare event. Note that these values are valid, whatever the return period, when the time window considered is the same as the return period.

We anticipate that comparisons with recorded strong motions will be difficult with such rare events. Frequency-magnitude distributions model the recurrence from all earthquakes falling within the magnitude-dependent completeness times. These distributions can be quite well constrained, at least for the low range of magnitudes where recurrence intervals of earthquakes are short with respect to the length of the historical catalogs (several hundreds of years). The recurrence model then enables the extrapolation to the upper range of magnitudes for which few data are available. Therefore, validation tests made based on the seismicity models may be more constrained than tests on ground-motion occurrences. To answer this question in the following sections, contributing earthquakes are identified in terms of locations and recurrence intervals. To avoid confusion, the term return period will be restricted to ground motions, and the term recurrence interval will be employed when dealing with earthquakes.

The Complex Link between Return Periods and Recurrence Intervals

Disaggregation in Recurrence Intervals

What are the recurrence intervals of the earthquakes contributing to the hazard at given return periods? Intuitively, recurrence intervals are assumed to be comparable to the return periods; for example, earthquakes participating at 475 yr would themselves have recurrence intervals of about 400–

500 yr. However, as several authors have already highlighted, seismic events contributing for a given return period are not necessarily characterized by similar recurrence intervals (Abrahamson, 2000; Bommer *et al.*, 2004). Applying the concept of disaggregation, already developed in magnitude, distance, and epsilon (Bazzurro and Cornell, 1999), to the recurrence intervals of earthquakes enables us to identify exactly the frequency of seismic events contributing at a given return period.

A disaggregation in recurrence intervals presents the same difficulties as disaggregation in terms of distances (Bazzurro and Cornell, 1999). In probabilistic calculations, areal source zones must be subdivided in subzones that can be approximated by point sources due to the use of an attenuation equation that employs hypocentral distance. The seismic rate attributed to a point source depends on the size of the subzone. To reduce computing time, most probabilistic hazard codes handle variable sizes of subzones; the longer is the source-site distance, the larger can be the surface represented by the point source. To perform a nonbiased disaggregation in recurrence intervals, the subzones used must have a unique size.

Contributing Recurrence Intervals for a Synthetic Seismicity Distribution

The disaggregation in recurrence intervals is presented for a synthetic seismicity distribution (Fig. 2a, fractal distribution; see Beauval *et al.* [2006b] for more details). In this case, the subdivision in space is fixed. Thus, the results are not dependent on the choices made. Each point source is characterized by a recurrence curve for magnitudes (Gutenberg–Richter with b -value of 1.0). The probabilistic seismic hazard is calculated using a minimum magnitude of 4.5, a maximum magnitude of 6.0, and a truncation of the

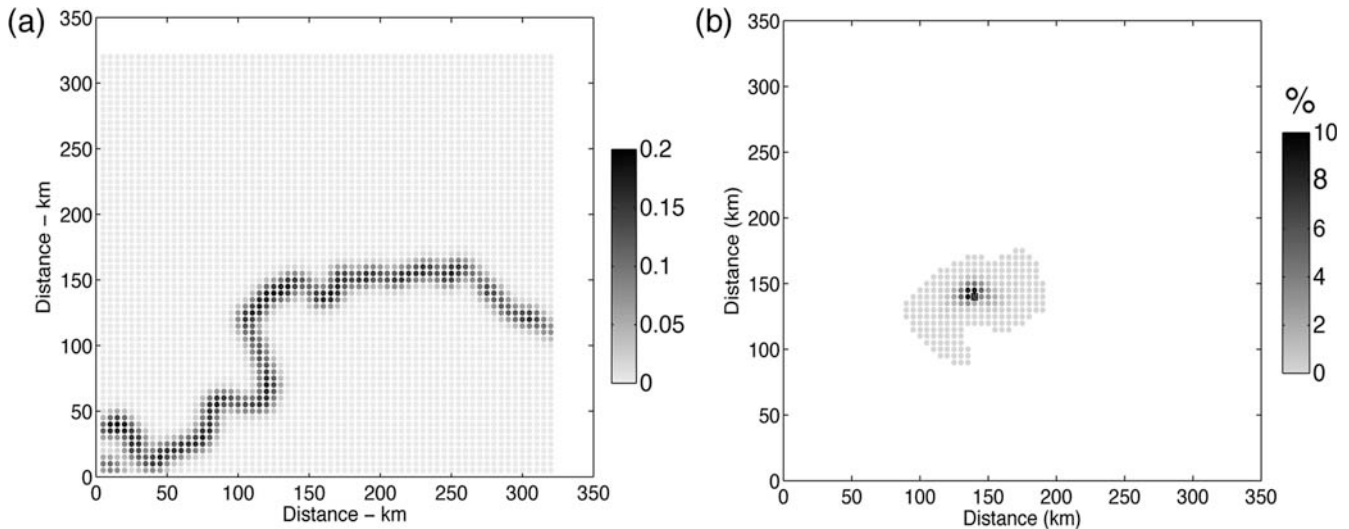


Figure 2. Synthetic example, grid of sources/sites: 5×5 km. (a) Seismic rate distribution of magnitudes $M \geq 3.0$, fractal dimension ~ 1.0 , overall occurrence rate 40 events with magnitude $M \geq 3$ per year. (b) Disaggregation in space, for the site (140,140) and the return period $T = 475$ yr (acceleration $A^* = 0.31g$).

ground-motion model predictions at $\pm 3\sigma$. By disaggregating the hazard in space, the spatial distribution of contributing point sources is obtained at the example site. At 475 yr (Fig. 2b), all contributing point sources are located within 50–60 km of the site. Disaggregations in recurrence intervals are displayed for several return periods, from 100 to 10,000 yr (Fig. 3a). Note that contributions are accumulated in bins equally spaced in logarithmic scale (see the legend) and expressed in percentage of the total hazard. As expected, if contributions per time unit are calculated (Fig. 3b), the jumps corresponding to the changes in the bin length disappear. However, the histograms in Figure 3a directly yield the contributions to the hazard due to recurrence interval ranges of the bins.

The results show that for short and long return periods, the range of time recurrences contributing is very large, from ~ 800 to $\sim 200,000$ yr. Although this result is not intuitive, it can be understood by going back to the core of the probabilistic computation: each earthquake, whatever its recurrence interval, has a nonzero probability of occurring in the next 50 yr, and might have a nonzero probability of generating a ground motion higher than the target level (due to the sigma of the ground-motion prediction equation). For the same distance, low magnitudes are much more numerous than large ones, but for large return periods ($\geq 5,000$ yr), this may be counterbalanced by the higher probability for large magnitudes to produce an acceleration higher than the target level (see, e.g., Reiter, 1990; Beauval and Scotti, 2004). Probabilities of all earthquakes are added, and the output cannot be linked easily to the inputs although all calculations are meaningful (contrary to the conclusions of Wang and Ormsbee, 2005). However, some observations are more intuitive (Fig. 3a). When the return period increases, the minimum recurrence interval contributing increases slightly, the contri-

bution of the low range of recurrence interval decreases, and the contribution of the upper range of recurrence interval increases. These features can be generalized, as will be shown in a real case.

Contributing Recurrence Intervals: Real-Data Example

The sample site is located in the Alps, at the border between France and Italy (Fig. 4). For this example, four source zones of the zoning delineated by Autran *et al.* (1998) are considered (see Table 1 and Beauval, Scotti, and Bonilla [2006] for more details). The source zones have been subdivided into square cells of 7×7 km. We checked that the approximation at the border of the source zones has a negligible impact on the hazard estimation at the site (located in zone 1). We also checked that the results are only slightly dependent on the size of the cells. The cell sizes are small enough to apply the point source hypothesis, but still meaningful for the assumption of the occurrence of moderate magnitudes. The main characteristics observed in the synthetic case are retained (Fig. 5a). For all return periods from 100 to 10,000 yr, a large range of recurrence intervals contributes significantly to the hazard: from $\sim 6,000$ to $\sim 400,000$ yr. The recurrence interval of 6,000 yr corresponds to the recurrence interval of magnitudes $M \geq 4.5$ for the cells of source zone 1 (corresponding to a mean recurrence interval of ~ 20 yr for an $M \geq 4.5$ anywhere inside the source zone). Again, when the return period increases, the contributions of sources characterized by large recurrence intervals also increase with respect to the contributions of sources characterized by low recurrence intervals. Larger magnitudes have on average larger recurrence intervals, and the disaggregation in magnitudes also shows a shift of the barycenter of contributions towards the upper bound

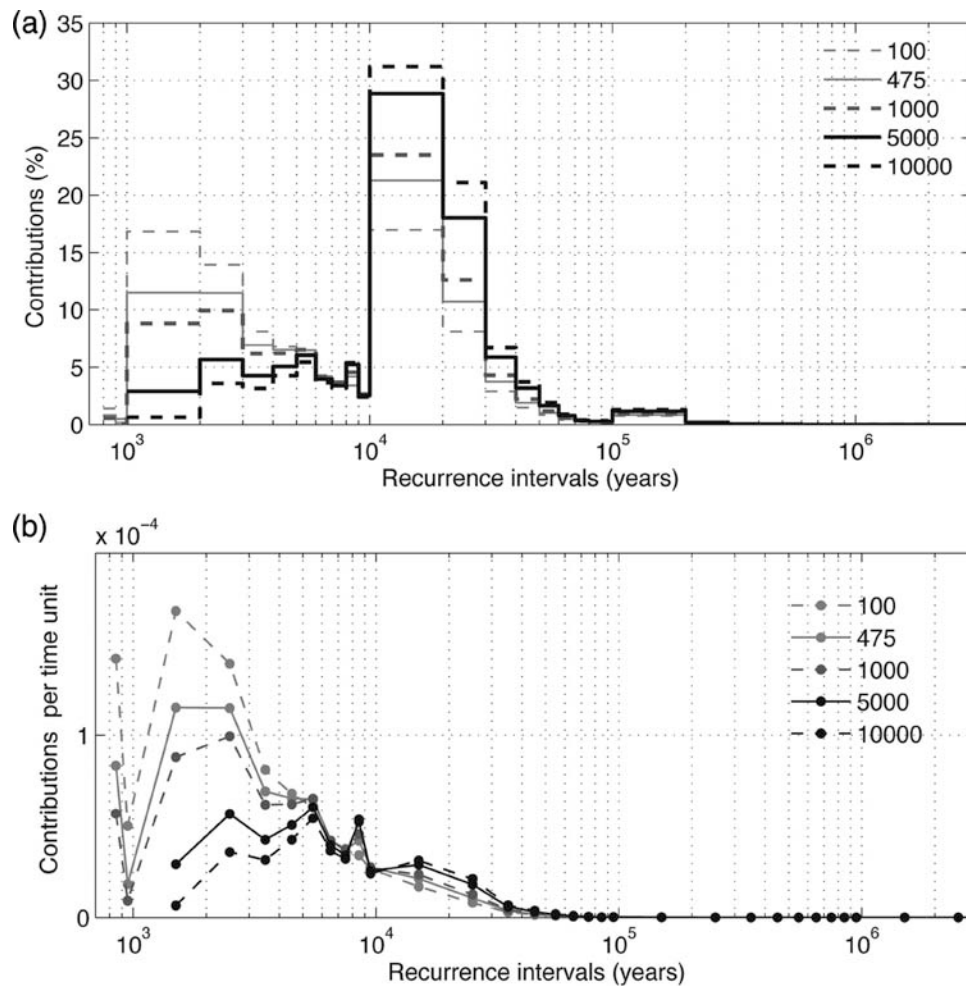


Figure 3. (a) Disaggregation of hazard in recurrence interval for five return periods (from 100 to 10^4 yr). Contributions are expressed in percentage of the total hazard. Bins are equally spaced in logarithmic scale (interval of 10^2 for values between 10^2 and 10^3 , 10^3 for values between 10^3 and 10^4 , 10^4 for values between 10^4 and 10^5 , and 10^5 for values between 10^5 and 10^6). Each horizontal segment delimits the boundaries of the bin (e.g., at 1000 yr, 9% of the hazard is due to recurrence intervals between 10^3 and 2×10^3 yr and 23% to recurrence intervals between 10^4 and 2×10^4 yr). (b) Contributions in (a) normalized by dividing by the bin lengths (per time unit).

of the magnitude range for increasing return periods (Fig. 5b).

On Validation Tests Based on Ground Motions

For identifying the recurrence intervals of contributing earthquakes, the recurrence curves of the seismic sources are of no use; point sources must be considered. The disaggregations show that the recurrence intervals of the contributing point sources are longer than the return periods of the target ground motions. Furthermore, the range of contributing recurrence intervals is large and roughly similar for all return periods between 100 and 10,000 yr. Although it might be easier to constrain seismicity models with observations, due to the length of the seismic catalogs, the validation test of probabilistic studies must be done on the final outputs (ground motions). Indeed, disaggregations show that only a subset of point sources contributes to the hazard and that

the link between inputs and outputs is rather complex. Directly comparing observed and calculated occurrences of ground motions is the most robust and efficient validation test of the probabilistic methodology, as Ordaz and Reyes (1999) showed. In the following, the validity domain of such a test is determined from simulations and applied to real data obtained at accelerometer sites in the French Alps, Greece, and southern California.

Difficulty of Constraining Probabilistic Predictions

Simulations of Poisson processes show that for processes characterized by low annual rates, the number of occurrences can vary greatly if short time windows are considered. The question to be addressed now is how long should the time window at the site be to ensure a meaningful estimation of the occurrence rate.

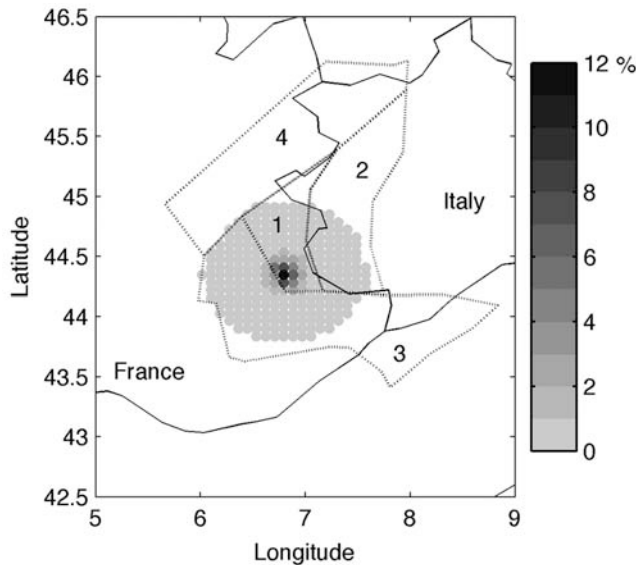


Figure 4. Probabilistic hazard study at the site (6.7; 44.3) in the French Alps: disaggregation in space for the return period 1000 yr. Contributions to the hazard are expressed in percentages. The point source contributing the most is located at the site. Dashed lines are seismic sources considered in the estimation (extracted from the zoning by Autran *et al.*, 1998), see Table 1.

Simulations: Minimum Time Windows versus Return Periods

A Poisson process with a return period 475 yr is simulated. As expected, the plot of the cumulative number of occurrences versus time shows a rather stable slope over time (Fig. 6). The mean annual rate is recomputed each time the event occurs by dividing the cumulated number of events by the total time elapsed (Fig. 6). For this sample run, the required time for the mean rate to be within $\pm 10\%$ of the theoretical value is around 33,000 yr. For different runs, this minimum time window, which ensures a value within a 10% uncertainty, is found to vary significantly. This dispersion can be taken into account by associating the length of the time window to the uncertainty of the occurrence rate.

The uncertainty of the occurrence rate is here the coefficient of variation (COV) (i.e., the standard deviation of the distribution divided by the mean and expressed in percentages). For a Poisson process, it is equal to the inverse of

the square root of the number of events N used:

$$\text{COV}(\lambda) = \frac{1}{\sqrt{N}}. \quad (2)$$

Running numerous simulations of a Poisson process characterized by a return period T and stopping each simulation once a fixed number of events N is reached, confirms equation (2) (simulations for $N = 10, 25,$ and 100 , see Fig. 7). Seven different return periods are considered ($T = 1$ month, 1 yr, 100, 475, 1000, 3000, and 10^4 yr). The COV on the occurrence rate λ is thus dependent only on the number of occurrences. The higher the number of events considered, the lower the uncertainty on the estimated rate (from $\text{COV} = 30\%$ for $N = 10$ to $\text{COV} = 10\%$ for $N = 100$). Moreover, the minimum time window required to ensure a rate with a given uncertainty can be evaluated, by computing for each simulation in this sample calculation, the total time length (from $t = 0$ to the time of the N th event). Mean values and standard deviations of time windows are displayed versus the return periods in Figure 8. Only the mean values will be used next.

Minimum time windows required to ensure the estimation of a reliable rate are listed in Table 2, for several return periods. For a Poisson process with return period of 1 yr, a minimum time window of 25 yr is required to ensure an estimated rate within 20% of the true rate. For a process with mean return period 475 yr, the minimum time window is 12,000 yr, again for an uncertainty of 20%. Note that this result is valid whatever the level of seismicity of the region. These results indicate that the comparison of predicted and observed occurrence rates at a unique observation site will be possible only for ground motions with very short return periods. The first accelerometers in the world were installed in the early 1930s (see Trifunac and Todorovska, 2001) and the first comprehensive networks in the 1960s, so the maximum observation time window is around 40 yr, like the station used by Ordaz and Reyes (1999). For a time window of ~ 40 yr, if the accepted level of uncertainty is 20%, the longest return period that can be considered for a comparison test is 1.6 yr, or the minimum annual rate is ~ 0.62 (Fig. 8). Accepting an uncertainty level of 30%, this minimum annual rate is ~ 0.25 (return period of 4–6 yr). Ordaz and Reyes (1999) compare predictions with observed annual rates from 0.03 to 0.6 (fig. 5 in their paper), based on a 35-yr observation time window. Note that although the lowest rates are not well constrained, the observations fit the calculated rates very well.

Table 1

Characteristics of Seismic Sources

Source	Seismic Rate $M \geq 4.5+$	b	M_{\max}
1	0.0680	0.86	6.0
2	0.1351	0.92	6.0
3	0.1154	1.06	6.0
4	0.0355	1.11	6.0

See Figure 4 and Beauval, Scotti, and Bonilla, 2006. For simplicity, maximum magnitudes are fixed to 6.0.

Application to Sites of the French Strong-Motion Network

The time window available is so short that the ground-motion range, where calculated rates can be considered meaningful, is expected to be low, corresponding to very frequent events. Nonetheless, the experiment is carried out. These conditions derived from simulations are applied

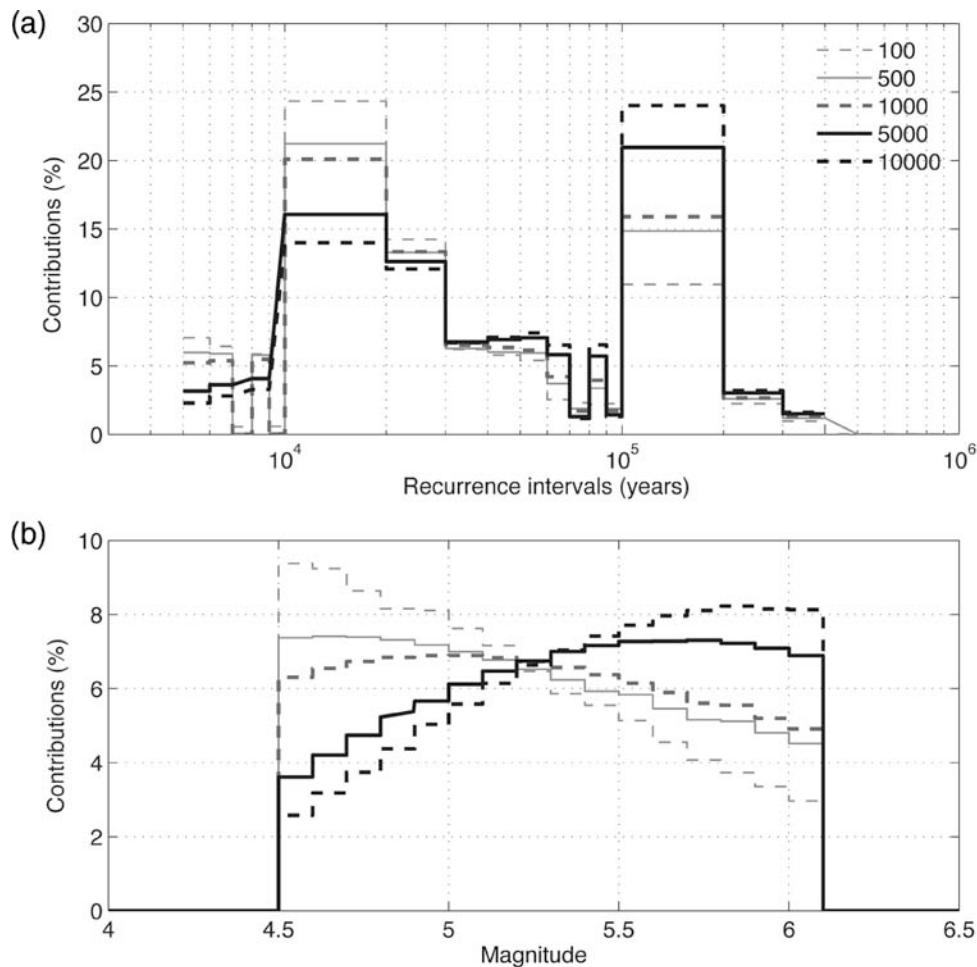


Figure 5. (a) Disaggregation in recurrence intervals for the hazard estimated at the site (6.7; 44.3) in the Alps for five return periods. Contributions are expressed in percentage of the total hazard. Bins are equally spaced in logarithmic scale (i.e., interval of 10^3 for values between 10^3 and 10^4 , 10^4 for values between 10^4 and 10^5 , and 10^5 for values between 10^5 and 10^6). (b) Disaggregation in magnitude; magnitude bin of 0.1 unit. Corresponding acceleration levels: 0.09g, 100 yr; 0.17g, 500 yr; 0.22g, 1000 yr; 0.36g, 5000 yr; 0.43g, 10,000 yr.

at the sites of the French strong-motion network (RAP, www-rap.obs.ujf-grenoble.fr/, last accessed January 2008; Péquegnat *et al.*, 2008). All the sites of the metropolitan network are analyzed. The first stations were installed in 1996. Note that a few older accelerometers have been installed for several decades at nuclear sites. However, the minimum detection threshold of these instruments is so high (around $0.01g$) that very few (if any) data have been recorded. At each RAP station, the empirical recurrence curve for accelerations is derived: cumulative occurrence rates versus accelerations. The accelerations higher than $0.0001g$ and associated with events having a magnitude larger than 2.0 are taken into account. One of the sites where the largest amount of data is available is a station located on rock in the southern Alps: station STET in Saint Etienne de Tinée (Fig. 9), installed since 1996. A curve similar to the Gutenberg–Richter curve for magnitudes is obtained (Fig. 10) with an exponential decrease of the rates with acceleration bending in the upper range. This deviation from a straight line indicates that the time window available is not long enough

to compute meaningful rates. This curve is exactly equivalent to a hazard curve, the output of a probabilistic study. The uncertainties on the observed rates (COV, equation 2) are also displayed in Figure 10. In considering rates with a maximum uncertainty of 30%, probabilistic predictions can be tested against observations in the narrow range (0.0001 – $0.001g$) levels, which are much lower than the levels of interest in earthquake engineering. Even if using a ground-motion prediction equation uniformly valid for a wide range of accelerations (e.g., from 0.0001 to $1.0g$), would it be reasonable to generalize the results of a comparison test at very low levels to higher acceleration levels?

Application to Sites with a Longer Recording History

As the acceleration range available in France is of little use for engineering studies, other stations with a longer recording history in more active regions could be considered for a similar analysis. Figure 11 depicts the ground-motion recurrence curve for two such example sites: El Centro in

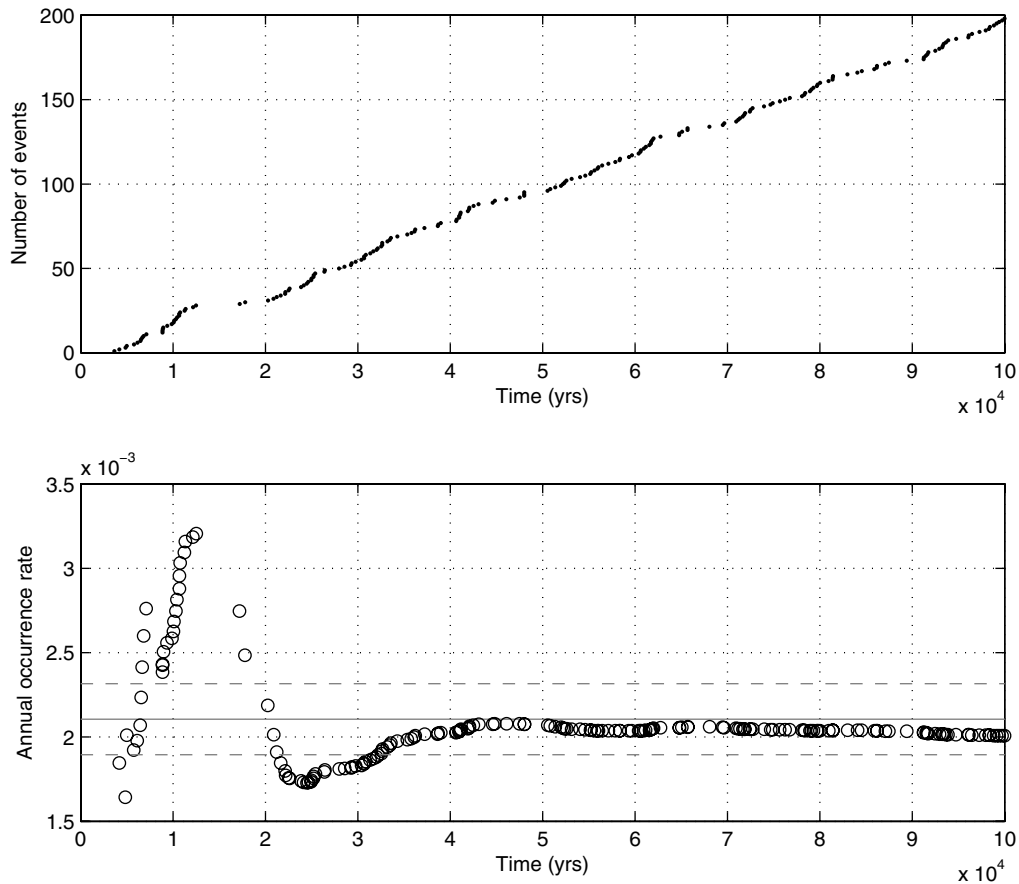


Figure 6. Simulation of a Poisson process with return period 475 yr. Upper: Cumulated number of occurrences versus time (yr). Lower: Corresponding mean annual rate, calculated each time the event occurs, versus time. Solid line is the theoretical mean rate; dashed lines are $\pm 10\%$ of the mean rate value.

southern California and Lefkada in western Greece. The El Centro site has been instrumented since 1934 and has recorded many significant earthquakes (see the Pacific Earthquake Engineering Research [PEER] strong-motion database for further details, <http://peer.berkeley.edu/smcat/>, last accessed January 2008). Accepting a maximum uncertainty of 30% on the rate, acceleration levels available for comparison studies reach 0.1g. The Lefkada site in Greece has been instrumented since 1973 (see the European Strong Motion database, www.isesd.cv.ic.ac.uk/ESD/frameset.htm, last accessed January 2008; Ambraseys *et al.*, 2004). A maximum uncertainty of 30% on occurrence rates yields acceleration levels again as high as 0.1g (Fig. 11). Moreover, strong-motion records at station Nocera Umbra, installed since 1977 in Italy, have also been analyzed. The rates of acceleration levels up to 0.2g can be estimated with a maximum 30% uncertainty. However, this station perhaps should not be used for a comparison test due to the inclusion of numerous aftershocks of the Umbria–Marche earthquake of 26th September 1997 (M_w 6.0). There are only a few sites in the world that have been instrumented for several decades. The analyses at El Centro and Lefkada station show that the maximum ac-

celeration level available for comparisons between predictions and observations is around 0.1g.

Compensating Short Time Windows by Spatial Aggregation

As shown previously, the most unbiased comparison test—comparing real recordings to predictions at one site—will be restricted to ground motions with a high frequency of occurrence. Because of this restriction, other tests must be explored and are briefly discussed here. Ward (1995) proposes the following: the region of interest is covered by a grid of sites, and the sites characterized by a similar probabilistic hazard value are grouped (they are characterized by a probability P of exceeding a given acceleration level in the next t yr). If P percent of the grouped sites have indeed seen an acceleration higher than the target level over t yr, the probabilistic prediction is validated. Ward (1995) applies this technique in the United States, and for each site, the historical acceleration catalog is calculated using the earthquake catalog (200 yr) and a ground-motion prediction equation. Now that more strong-motion records are available, it would be worth applying this test to real data, avoiding the need for

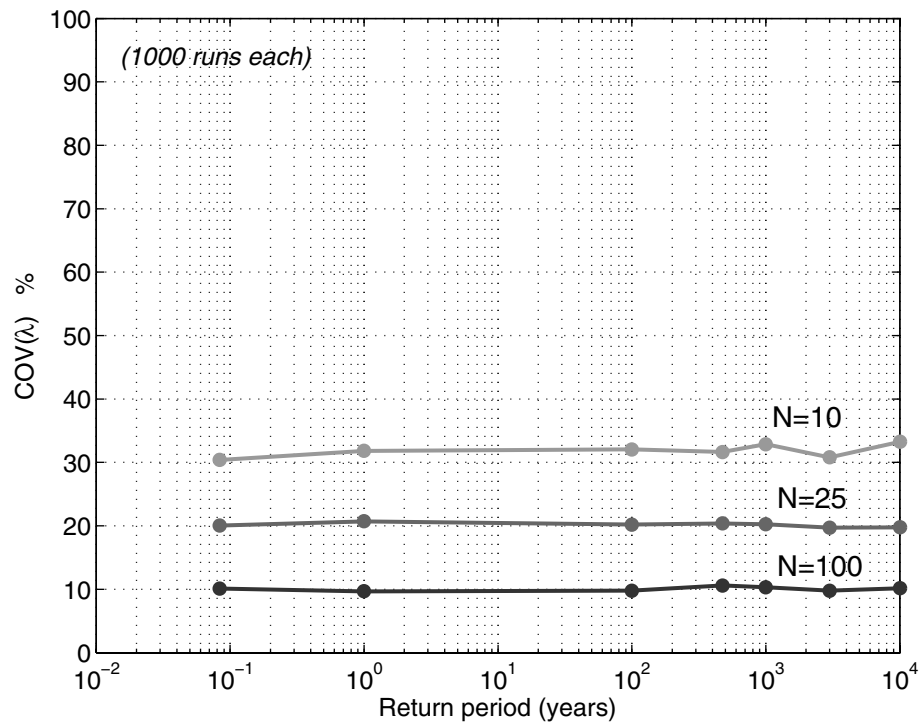


Figure 7. Simulations of Poisson processes for return periods from 1 month to 10,000 yr; each value relies on 1000 runs. Uncertainty on the estimated occurrence rate λ versus return periods, $COV = S.D./MEAN$, considering sequences with 10, 25, and 100 occurrences. The corresponding time windows are displayed in Figure 8.

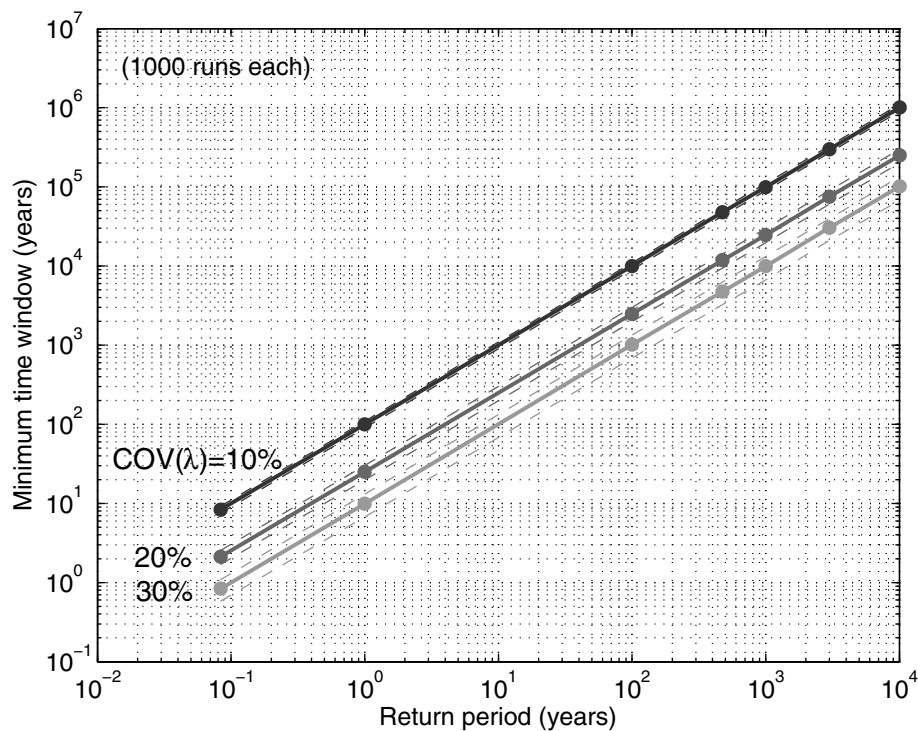


Figure 8. Simulations of Poisson processes for different return periods (see Fig. 7 and legend). Minimum time windows required for ensuring a given uncertainty level on the estimated rate λ (COV), versus return period. Solid line, mean values; dashed lines, standard deviations.

Table 2

Minimum Observation Time Window of a Poisson Process with Return Period T to Ensure a Rate with 20% Uncertainty

Return Period T (yr)	Minimum Time Window (yr)
1 month	2
1	25
475	12,000
3000	75,000
10,000	250,000

a ground-motion prediction equation. However, a major difficulty in conducting such a study will be local site effects at each station, a problem that was not encountered in Ward’s study, as both the probabilistic estimates and the accelerations were calculated with the same ground-motion model. Another major problem will be the required number of instrumented sites. If the network has been installed for 15 yr, and if considering ground motions with a 475-yr return period, 800 sites would be necessary for an estimation of the rates with a maximum uncertainty of 20% (see Table 2). Therefore, comparison tests will be possible only for return periods lower than the return periods of interest in the engineering studies. Moreover, this test relies on the ergodic assumption (Anderson and Brune, 1999), and the aggregation of sites with similar probabilistic hazard values to estimate the probability of exceedance can be considered as a bias. Nevertheless, these numbers, though large, do suggest that such statistical tests should be performed in countries where dense strong-motion networks are installed (e.g., Japan and Taiwan) and should be considered as complementary to the tests focusing on one site, as different acceleration ranges will be addressed.

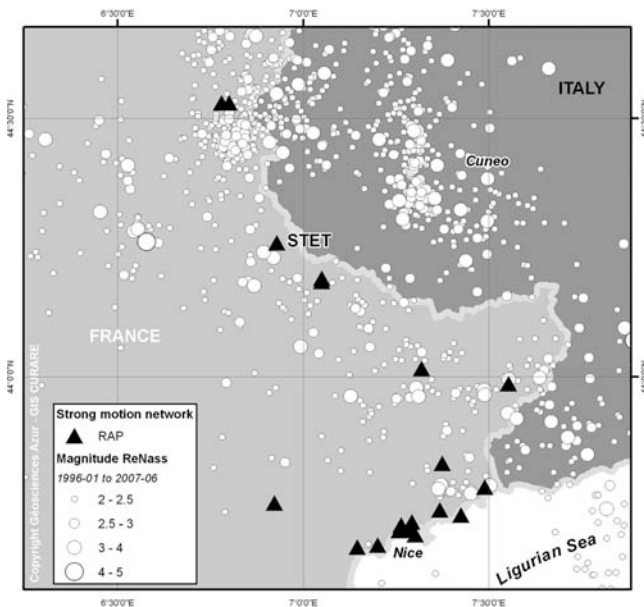


Figure 9. Seismicity map over the time period 1996–2007. Site under study is RAP/TGRS station STET.

Conclusions

This study demonstrates that the comparisons between observations and predictions can provide only limited constraints on probabilistic seismic hazard estimates. Such comparisons can be performed for the source (earthquake occurrences) or for the ground motion. As the latter corresponds to the hazard itself, tests on ground motion are more relevant than tests on earthquake occurrence. Based on the simple simulation of Poisson processes, the minimum time window required for estimating meaningful ground-motion occurrence rates is quantified. As expected, these time windows are very long for the ground motions of interest in engineering studies (return periods of 475 yr and longer). The best validation test, comparing observations and predictions at a site, will remain out of reach for these return periods. For example, accepting a maximum uncertainty of 20% on the occurrence rate of accelerations, a time window of 12,000 yr is required for the return period of 475 yr. Applications of the method at several sites in France, Greece, and California show that, at best, ground accelerations up to 0.1g can be considered (accepting a 30% uncertainty threshold). A comparison test carried out at low levels would need to be extrapolated to higher levels. Such extrapolation techniques need further study to be validated. Since the need for con-

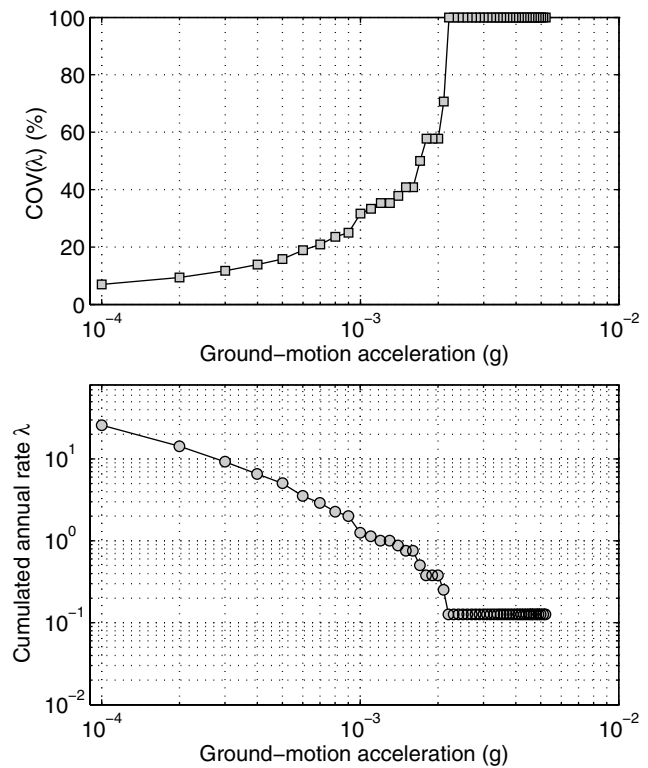


Figure 10. Analysis of recorded ground motions at station STET over the time period 1996–2005. Upper: Uncertainty on the occurrence rate versus acceleration (COV, equation 2). Lower: Cumulated annual rate versus acceleration (peak ground acceleration).

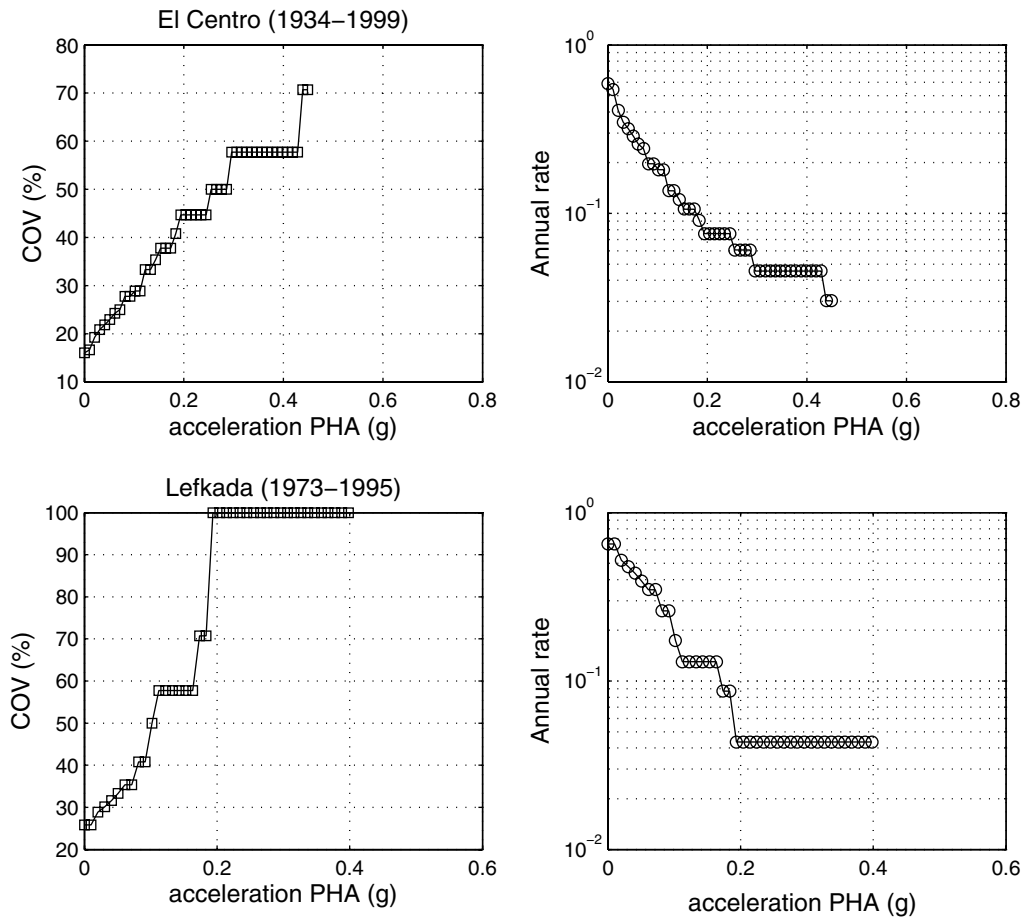


Figure 11. Analysis of recorded ground motions at two stations: El Centro in southern California (top) and Lefkada in Greece (bottom). Left: Uncertainty on the occurrence rate versus acceleration (COV, equation 2). Right: Cumulated annual rate versus acceleration (peak ground acceleration).

straining hazard estimates is urgent, other tests must be explored for taking advantage of available observations. For example, Ward's (1995) method could be applied in regions with dense accelerometer networks. His results will help in constraining the hazard estimates, although there will be a bias due to the nonindependence of ground motions at sites affected by the same earthquakes. Since comparing ground-motion occurrence rates with observation will remain difficult, existing methods focusing on testing modeled earthquake occurrences (in magnitude and space) against observations remain essential.

Acknowledgments

The comments from Associate Editor Julian Bommer and from John Douglas and an anonymous reviewer were really constructive and helpful for improving the manuscript, and we are very grateful to them. We are also thankful to Matt Yedlin for careful proofreading of the manuscript and for improving the English. A special thanks goes to John Douglas for his help in collecting part of the data and providing interesting papers during the revision of the manuscript. Finally, we are grateful to Christophe Maron and Didier Brunel for operating and archiving data from the southeastern RAP stations. This work has been partially supported by the Quantitative

Seismic Hazard Assessment (QSHA) project from the Agence Nationale de la Recherche under the Contract Number ANR-05-CATT-011.

References

- Abrahamson, N. A. (2000). State of the practice of seismic hazard evaluation, *GeoEng 2000*, 1, Melbourne, Australia, 19–24 November 2000, 659–685.
- Ambraseys, N. N., P. Smit, J. Douglas, B. Margaritis, R. Sigbjörnsson, S. Olafsson, P. Suhadolc, and G. Costa (2004). Internet site for European strong-motion data, *Boll. Geofis. Teorica Appl.* **45**, 3, 113–129.
- Anderson, J. G., and J. Brune (1999). Probabilistic seismic hazard analysis without the ergodic assumption, *Seism. Res. Lett.* **70**, 1, 19–28.
- Anooshehpour, A., J. N. Brune, and Y. Zeng (2004). Methodology for obtaining constraints on ground motion from precariously balanced rocks, *Bull. Seismol. Soc. Am.* **94**, no. 1, 285–303.
- Autran, A., J. L. Blès, Ph. Combes, M. Cushing, P. Dominique, C. Durouchoux, J. C. Gariel, X. Goula, B. Mohammadioun, and M. Terrier (1998). Probabilistic seismic hazard assessment in France. Part I: Seismotectonic zonation, in *Proceedings of the 11th European Conference on Earthquake Engineering*, 6–11 September 1998, Paris, France.
- Bazzurro, P., and C. A. Cornell (1999). Disaggregation of seismic hazard, *Bull. Seismol. Soc. Am.* **89**, no. 2, 501–520.
- Beauval, C., and O. Scotti (2004). Quantifying sensitivities of PSHA for France to earthquake catalog uncertainties, truncation of ground-

- motion variability, and magnitude limits, *Bull. Seismol. Soc. Am.* **94**, 1579–1594.
- Beauval, C., S. Hainzl, and F. Scherbaum (2006a). Probabilistic seismic hazard estimation in low-seismicity regions considering non-Poissonian seismic occurrence, *Geophys. J. Int.* **164**, 543–550.
- Beauval, C., S. Hainzl, and F. Scherbaum (2006b). The impact of the spatial uniform distribution on probabilistic seismic hazard assessment, *Bull. Seismol. Soc. Am.* **96**, 2465–2471.
- Beauval, C., O. Scotti, and L. F. Bonilla (2006). The role of seismicity models in probabilistic seismic hazard estimation: comparison of a zoning and a smoothing approach, *Geophys. J. Int.* **165**, 584–595.
- Bommer, J. J. (2006). Re-thinking seismic hazard mapping and design return periods, in *First European Conference on Earthquake Engineering and Seismology*, Geneva, Switzerland, 3–8 September 2006, Paper 1304.
- Bommer, J. J., and R. Pinho (2006). Adapting earthquake actions in Eurocode 8 for performance-based seismic design, *Earthq. Eng. Struct. Dyn.* **35**, 39–55.
- Bommer, J., F. Scherbaum, F. Cotton, H. Bungum, and F. Sabetta (2004). Uncertainty analysis of strong motion and seismic hazard by R. Sigbjörnsson and N. N. Ambraseys, discussion, *Bull. Earthq. Eng.* **2**, 261–267.
- Cornell, C. A. (1968). Engineering seismic risk analysis, *Bull. Seismol. Soc. Am.* **58**, 1583–1606.
- Cornell, C. A., and S. R. Winterstein (1988). Temporal and magnitude dependence in earthquake recurrence models, *Bull. Seismol. Soc. Am.* **78**, no. 4, 1522–1587.
- Dominique, P., A. Autran, J. L. Blès, D. Fitzenz, F. Samarcq, M. Terrier, M. Cushing, J. C. Gariel, B. Mohammadioun, Ph. Combes, C. Durouchoux, and X. Goula (1998). Part two: probabilistic approach, seismic hazard map on the national territory (France), in *Proc. of the 11th ECEE*, 6–11 September 1998, Paris, France.
- Douglas, J. (2003). Earthquake ground motion estimation using strong-motion records: a review of equations for the estimation of peak ground acceleration and response spectral ordinates, *Earth Sci. Rev.* **61**, 43–104.
- Fujiwara, H., S. Kawai, S. Aoi, T. Kunugi, T. Okumura, T. Ishii, Y. Hayakawa, N. Morikawa, K. Kobayashi, M. Ooi, S. Senna, and N. Okumura (2005). Tech. Note 275, A study on probabilistic seismic hazard maps of Japan, National Research Institute for Earth Science and Disaster Prevention (NIED).
- Gutenberg, G., and C. F. Richter (1944). Frequency of earthquakes in California, *Bull. Seismol. Soc. Am.* **34**, 185–188.
- Humbert, N., C. Durouchoux, and E. Viallet (2007). Confrontation des études probabilistes d'aléa sismique aux observations instrumentales, in *VIIth National Conference on Earthquake Engineering*, Chatenay-Malabry, France, 4–6 July 2007, Paper 60, 8 pp.
- Labbé, P. (2007a). Sur l'évaluation du risque sismique en France à partir des données d'aléa et de fragilité, in *VIIth National Conference on Earthquake Engineering*, Chatenay-Malabry, France, Paper 61, 4–6 July 2007, 8 pp.
- Labbé, P. (2007b). Evaluation du risque sismique observe historiquement en France, in *VIIth National Conference on Earthquake Engineering*, Chatenay-Malabry, France, 4–6 July 2007, Paper 63, 8 pp.
- Labbé, P. (2007c). Traitement statistique de données de sismicité historique et événements extrêmes, in *VIIth National Conference on Earthquake Engineering*, Chatenay-Malabry, France, 4–6 July 2007, Paper 62, 8 pp.
- Marin, S., J. P. Avouac, M. Nicolas, and A. Schlupp (2004). A probabilistic approach to seismic hazard in metropolitan France, *Bull. Seismol. Soc. Am.* **94**, 2137–2163.
- Martin, Ch., P. Combes, R. Secanell, G. Lignon, D. Carbon, A. Fioravanti, and B. Grellet (2002). Rapport GEOTER GTR/MATE/0701-150, Révision du zonage sismique de la France: etude probabiliste, under the supervision of the Groupe d'Etude et de Proposition pour la Prévention du risque sismique en France and the Association Française du Génie Parasismique (in French).
- McGuire, R. K. (1979). Adequacy of simple probability models for calculating felt-shaking hazard, using the Chinese earthquake catalog, *Bull. Seismol. Soc. Am.* **69**, 877–892.
- Musson, R. M. W. (2004). Objective validation of seismic hazard source models, in *13th world Conference on Earthquake Engineering*, Vancouver, B.C., Canada, 1–6 August 2004, Paper 2492, 11 pp.
- Ordaz, M., and C. Reyes (1999). Earthquake hazard in Mexico City: observations versus computations, *Bull. Seismol. Soc. Am.* **89**, no. 5, 1379–1383.
- Péquegnat, C., P. Guéguen, D. Hatzfeld, and M. Langlais (2008). The French Accelerometric Network (RAP) and National Data Center (RAP-NDC), *Seism. Res. Lett.* **79**, no. 1, 79–89.
- Reiter, L. (1990). *Earthquake Hazard Analysis: Issues and Insights*, Columbia University Press, New York.
- Sollogoub, P., P.Y. Bard, B. Hernandez, W. Jalil, P. Labbé, P. Mouroux, and E. Viallet (2007). Rapport du groupe de travail "Zonage", Association Française de génie Parasismique (AFPS), 58 pp. (in French, available on request).
- Tormann, T., M. K. Savage, and M. Stirling (2004). Dynamic seismic hazard model for New Zealand (Abstract S13A-1029), *AGU Fall Meeting*, San Francisco, California, S13A-1029.
- Trifunac, M. D., and M. I. Todorovska (2001). Evolution of accelerographs, data processing, strong motion arrays and amplitude and spatial resolution in recording strong earthquake motion, *Soil Dyn. Earthq. Eng.* **21**, 537–555.
- Viallet, E., N. Humbert, A. Courtois, C. Durouchoux, and P. Sollogoub (2007). Une technique d'actualisation Bayésienne pour traiter les incertitudes épistémiques dans une évaluation probabiliste de l'aléa sismique, in *VIIth National Conference on Earthquake Engineering*, Chatenay-Malabry, France, 4–6 July 2007, Paper 78, 8 pp.
- Wang, Z., and L. Ormsbee (2005). Comparison between probabilistic seismic hazard analysis and flood frequency analysis, *EOS* **86**, no. 5, 45–47.
- Ward, S. (1995). A multidisciplinary approach to seismic hazard in southern California, *Bull. Seismol. Soc. Am.* **84**, 1293–1309.
- Wesnousky, S. G. (1994). The Gutenberg-Richter or characteristic earthquake distribution, which is it?, *Bull. Seismol. Soc. Am.* **84**, 1940–1959.
- Working Group on California Earthquake Probabilities (WGCEP) (2003). Earthquake probabilities in the San Francisco Bay region: 2002 to 2031, *U.S. Geol. Surv. Open-File Rept. 03-214*.
- Youngs, R. R., and K. J. Coppersmith (1985). Implications of fault slip rates and earthquake recurrence models to probabilistic seismic hazard estimates, *Bull. Seismol. Soc. Am.* **75**, 939–964.
- Géosciences Azur
Institut de Recherche pour le Développement (IRD)
250 Rue Albert Einstein
06560 Valbonne, France
beauval@geoazur.unice.fr
(C.B.)
- Laboratoire de Géophysique Interne et Tectonophysique (LGIT)
BP 53
38041 Grenoble Cedex 9, France
(P.-Y.B., P.G.)
- GeoForschungsZentrum Potsdam
Telegrafenberg
14473 Potsdam, Germany
(S.H.)